BENTHAM OPEN

CrossMark

The Open Automation and Control Systems Journal

Content list available at: www.benthamopen.com/TOAUTOCJ/

DOI: 10.2174/1874444301811080025, 2018, *10*, 25-40

RESEARCH ARTICLE

Modelling and Reliability Analysis of Multi-source Renewable Energy Systems Using Deterministic and Stochastic Petri Net

El-kadi Hellel[1], Samir Hamaci[2,*] and Rezki Ziani[1]

[1] *Department of electronics of Tizi-Ouzou, Tizi-Ouzou, Algeria*
[2]*ECAM-EPMI, 13 Boulevard de l'Hautil, Cergy-Pontoise, 95092, Paris, France*

Received: January 10, 2018 Revised: October 11, 2018 Accepted: October 15, 2018

Abstract: In this paper, the energy systems based on renewable resources are studied. The purpose is to make an analysis of the dynamic behavior of the component elements of these systems in order to evaluate the performance related to their reliability and availability. Our approach is based on the use of Deterministic and Stochastic Petri Nets, to establish a model to extract performance with the goal to define subsequently a tolerant control process fault reconfigurable to limit risks unavailability.

Keywords: Modelling, Petri Nets, Performance evaluation, Renewable energy, Reliability, Simulation.

1. INTRODUCTION

With the energy challenges of today, the use of Multi-Source Renewable Energy Systems [1] [2] appears as a potential solution for the production of electricity on a large scale. These systems combine different sources (wind, PV, biomass, geothermal ...) and are characterized among other things by the diversity of elements that constitute the Mechanical elements (blades, actuators, *etc.*), chemical (battery) electrical (generators, converters) and computer (control and supervision program). These multiples components give these systems a complex character and make them quite difficult to study. The evaluation of their dependability (reliability, availability ...) is a major concern, because of the heterogeneity of their components and especially the demands of the energy market.

The methods of assessing the dependability in these fields (mechanical, electrical engineering, chemistry and computer science, ...) are indeed very different from each other. To date, there is no technique to quantify the reliability and availability of such systems. To overcome this problem, solutions need to be made to ensure continuity of service and optimum reliability of operations provided by these systems. The aim is to minimize the risks of defects or incidents which create a system downtime, thus intruding stocks and energy supply. In this article, we focus on the study of the dynamic behavior of these systems in order to make a subsequent quantitative analysis to evaluate their reliability in a model based on Petri nets. These graphs [3] introduced by Carl Adam Petri in 1962 [4], are powerful in modeling Discrete Event Systems [5]. These are defined by discrete state spaces where all state variables take their values in a countable set. The choice of this modeling tool is justified by the discrete nature of the state of system to be studied (functioning and failure).

Specifically, we use a category of Petri net which models the stochastic phenomenon, represented by the appearance of failures in the Multi-Source Renewable Energy Systems. These graphs are known as Deterministic and Stochastic Petri Nets (DSPN) [6], [7].

In the literature, to our knowledge, there are very few works that are interested in the qualitative and quantitative analysis of multi-source energy based Petri net systems. In [8], the authors propose a Petri net-based modeling for better

* Address correspondence to this author at the ECAM-EPMI, 13 Boulevard de l'Hautil, Cergy-Pontoise, 95092 , Paris, France, Tel: +33(0)130756931; E-mail: s.hamaci@ecam-epmi.fr

energy management of a multi-source power system consisting of a photovoltaic source (PV), a storage battery the classic grid. The authors in a study [9] proposed a stochastic Petri net based modeling for the management of energy to power a server set while taking into account their frequency of operation and the number of servers in idle state. In a study [10] the authors proposed a method to quantify and improve the performance of multi-source energy systems, using a PN graph. The work presented in [11] deals with the energy management of a photovoltaic based power station. This power station includes storage units with batteries for long-term energy supply and ultra-capacitors for fast dynamic power regulation. According to the availability of the primary source, the level of the stored energy and the request from the grid operator, the authors have defined three main operating modes for this system with a particular modeling tool: Petri nets. For each operating mode, an energy management algorithm has been designed in order to calculate the energy dispatching of an adjustable power margin for the storage units.

In this work, the DSPN is used to model the behavior related to the dynamic evolution of these systems to extract, by simulation, the instant of passage from the state of functioning towards to a state of breakdown and vice versa, noting that these moments are the time references that will be used to quantify the reliability and availability of these systems. Knowing that this reliability corresponds to the probability for a system to fulfill a required function during a period from 0 to t_1 [12], and availability is the probability that a repairable system operates in an interval from t_1 to t_2 [12].

This paper is organized as follows: after a general introduction describing the context of this work, the DSPN which is used for modeling of multi-source energy systems is presented in Section 2. The model governing the evolution of the functional and dysfunctional behavior of these systems is presented in Section 3. The performance evaluation using the simulation of these systems on quantifying the reliability is the subject of Section 4, this is followed by a subsequent analysis of results simulation before concluding this work.

2. DETERMINISTIC STOCHASTIC PETRI NET (DSPN)

This section presents the Deterministic and Stochastic Petri Nets (DSPN) that will be used for modeling of hybrid systems to renewable energy sources with the purpose to analyse the reliability of this systems. These graphs are defined as 11-tuple (P, T, I, O, MO, H, N, G, W, d, e), where P is a finite set of places. T is the finite set of transitions partitioned into three subsets: one subset of stochastic transitions T_e, where their firing follows stochastic law, a subset of deterministic transitions T_d and a subset of T_i immediate transitions. The set of arcs is divided into two subsets: a subset classical arcs: I is the set of arcs from the place *p* to transition *t*, and Y is the set of outgoing arcs showing from transition *t* to place *p*. H corresponds to the subset of inhibitor arcs. N is the weight of arcs on classical and inhibitor arcs. The initial state of DSPN is designated by M_o and the amount of tokens in place p_i is denoted by M (p_i). In DSPN, the places are represented by circles and the transitions by bars. Immediate transitions are presented by black bars and the deterministic transitions by filled rectangles and the stochastic transitions by empty rectangles. Durations ith firing *d* are represented in the following way: the exponential transition follows the form $\lambda e^{-\lambda t}$ with $t \in [0, +\infty[$ and the immediate transition *t*, $t \in [0, +\infty[$, deterministic transition $\delta(t-d)$, $t \in [0, +\infty[$, $d \neq 0$. The immediate transitions have priority over other transitions. In case of conflict between immediate transitions, the transition that has the highest priority e will be fired first, while the default priorities are equal to one. If two transitions are of the same priority, we will associate each immediate transition with a natural number (weight) represented by W, while its role is to resolve conflicts in a probabilistic law. Inhibitor arcs are represented by arcs which end by a small circle.

The use of inhibitor arcs increases the capacities of modelling and the property of a DSPN. If a place *p* and a transition *t* are connected by an Inhibitors arc with a weight N, transition *t* cannot be fired except if the marking of place *p* is lower than N. However, if a place *p* and a transition *t* are connected by a classical arc with a weight N, the transition *t* can be fired if the marking of the place *p* is greater than or equal to N. The main difference is when the firing of a transition *t* removes tokens in place *p* when are connected by a classical arc, while no token movement will take place in the case of inhibitor arcs. In addition to the symbols presented before, one will add the last symbol G which is a function of activation of the transitions.

3. MODELLING OF HYBRID RENEWABLE ENERGY SYSTEMS

3.1. Energy System Mono-source with Wind Turbine

This system consists of a wind turbine, connected to a DC bus through an AC/DC converter. The DC bus is

connected into a Load through an inverter (Fig. **1a**). The functional and dysfunctional model DSPN of this system is depicted in Fig. (**1b**).

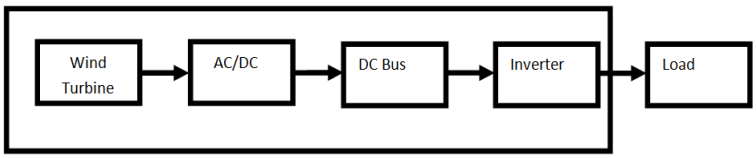

Fig. (1a). Mono-source energy system with wind turbine.

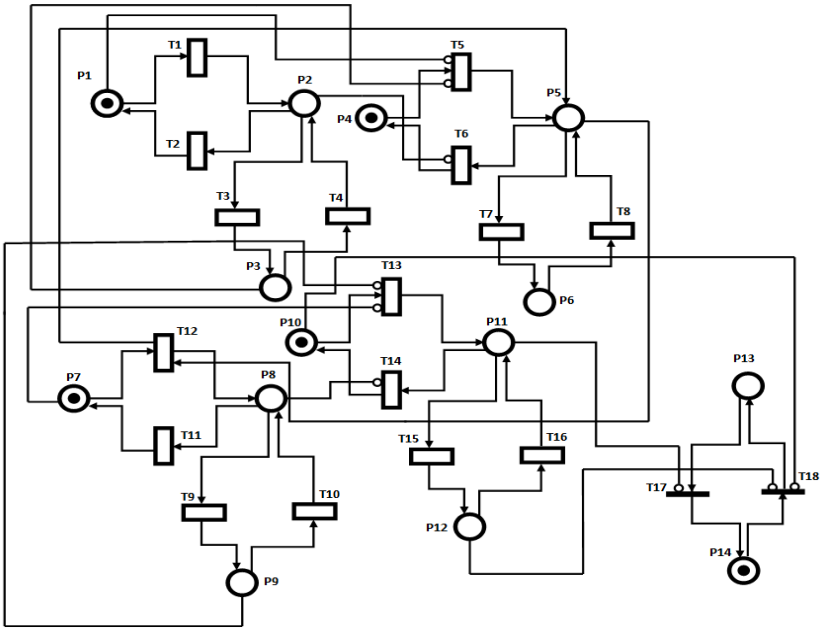

Fig. (1b). DSPN of a Mono-source energy system with wind turbine.

The Interpretation of places and transitions of this DSPN is given in Table **1** and Table **2** respectively. In Fig. (**1b**), we show that a system containing only wind turbine source is in a wait state (p_1) or breakdown state (p_3), the AC/DC converter, Inverter and the DC bus are stagnated in their wait states (p_4, p_{10}), and in the free state (p_7), the load will remain disconnected (p_{14}). The firing of transition t_1 will allow tokens of place p_1 to pass towards place p_2, that means that the wind turbine passes from the wait state towards the operating state, represented by the place p_2. The AC/DC converter, Inverter and DC bus will also pass them towards the operating condition in an occupied state p_5, p_{11}, p_8 respectively. This passage will influence directly the load which will pass towards the state connected p_{13}. If the wind turbine is in the wait state or of breakdown and the DC bus is in a breakdown state or the AC/DC converter is in a breakdown state, the oad will be automatically disconnected.

Table 1. Interpretation of places of the model DSPN depicted in Fig. (1b).

Place	Meaning
P1	Wait state of the wind turbine
P2	Operating state of the wind turbine
P3	Breakdown State of the wind turbine
P4	Wait state of AC/DC converter
P5	Operating condition of AC/DC
P6	Breakdown State of AC/DC converter
P7	DC bus is free (vacuum)
P8	DC bus is occupied
P9	DC bus is in a breakdown state
P10	Wait state of Inverter

(Table 1) contd.....

Place	Meaning
P11	Functional State of Inverter
P12	Breakdown State of Inverter
P13	Load is in connected state
P14	Load is in disconnected state

Table 2. Interpretation of transitions of the model DSPN depicted in Fig. (1b).

Transition	Type	Meaning
T1	stochastic	Passage of wait state towards the functional state of the wind turbine
T2	stochastic	Return of the wind turbine of the functional state towards the wait state
T3	stochastic	Passage of the wind turbine towards the breakdown state
T4	stochastic	Repair of the wind turbine
T5	stochastic	Passage of wait state towards the functional state of the AC/DC converter
T6	stochastic	Return of the AC/DC converter of the functional state towards the wait state
T7	stochastic	Passage of AC /DC converter towards the breakdown state
T8	stochastic	Repair of the AC/DC converter
T9	stochastic	Passage of DC bus towards the breakdown state
T10	stochastic	Repair of the DC bus
T11	stochastic	Return of the DC bus of the state occupied towards the state of vacuum
T12	stochastic	Passage of DC bus of the state of vacuum towards the occupied state of DC Bus
T13	stochastic	Passage of Inverter towards the functional state
T14	stochastic	Return of Inverter towards the rest state
T15	stochastic	Passage of Inverter of functional state towards the breakdown state
T16	stochastic	Repair of Inverter
T17	immediat	Desactivation of the Load
T18	immediat	Activation of the Load

3.2. Energy System Mono-source with Photovoltaic Module

This energy system contains only photovoltaic module (PV) connected directly to the DC bus and in its turn with a Load using an Inverter (Fig. **2a**). The functional and dysfunctional model of this system is represented by the DSPN depicted in Fig. (**2b**).

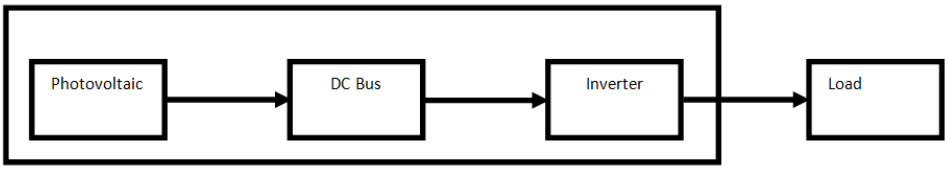

Fig. (2a). Mono-source Energy System with Photovoltaic module (PV).

In Fig. (**2b**), the token in place p modelling the wait state of photovoltaic and which is connected directly to the DC bus, also in the free state (p_5), and Inverter which is in the wait state (p_6) indicates that the Load is disconnected (p_{10}). The activation of transition t_1 will push the photovoltaic module to function p_1. This operation will influence the DC bus which will pass from the state of vacuum towards the occupied state (p_4) and Inverter towards the functional state (p_7). The token which is in place p_{10} passes towards the connect state (p_9) after the firing of the transition t_{14}. If the Photovoltaic module or the DC bus or Inverter is in a breakdown state, like represented in Fig. (**2b**) by the places p_1, p_3 and p_8, the Load will remain disconnected.

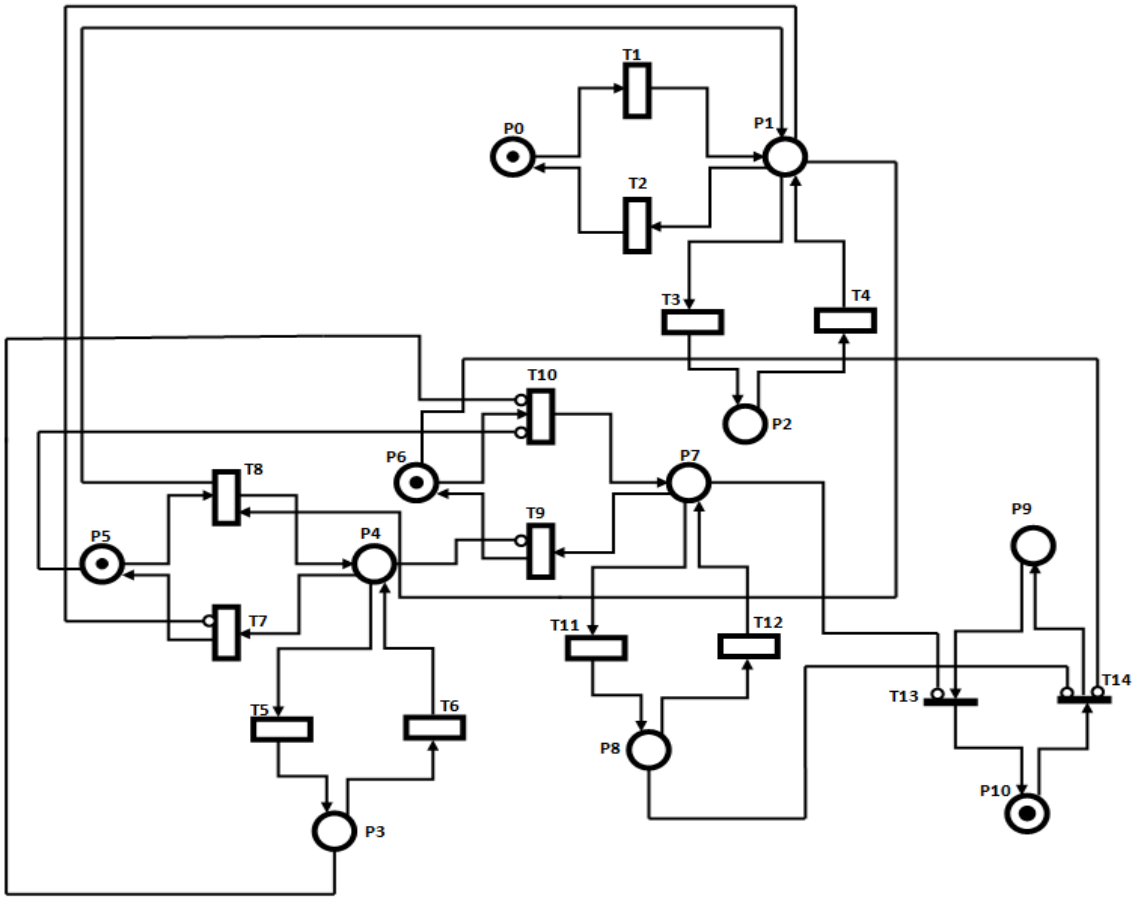

Fig. (2b). DSPN of a Mono-source energy system with photovoltaic module.

Table 3. Interpretation of places of the model DSPN depicted in Fig. (2b).

Place	Meaning
P0	Photovoltaic is in wait state
P1	Photovoltaic is in operating condition
P2	Photovoltaic is in a breakdown state
P3	DC bus is breakdown
P4	DC bus is occupied
P5	DC bus is in free state (vacuum)
P6	Inverter is in the wait state
P7	Inverter is in the operating condition
P8	Breakdown state of Inverter
P9	Load is connected
P10	Load is disconnected

Table 4. Interpretation of transitions of the model DSPN depicted in Fig. (2b).

Transition	Type	Meaning
T1	stochastic	Photovoltaic Passage of wait state towards the functional
T2	stochastic	Return of photovoltaic of the functional state towards the wait state
T3	stochastic	Passage towards the breakdown state of the Photovoltaic module
T4	stochastic	Repair of the Photovoltaic module
T5	stochastic	Passage towards the breakdown state of the DC bus
T6	stochastic	Repair of the DC bus
T7	stochastic	Return of the DC bus of the state occupied towards the vacuum state

(Table 4) contd.....

Transition	Type	Meaning
T8	stochastic	Passage of the DC bus of the state of vacuum towards the occupied state
T9	stochastic	Return of Inverter towards the wait state
T10	stochastic	Passage Inverter of the wait state towards the functional state
T11	Stochastic	Passage of Inverter towards the state of breakdown
T12	Stochastic	Repair of Inverter
T13	immediat	Passage towards the disconnected state of the Load
T14	immediat	Passage towards the connected state of the Load

3.3. Multi-source Renewable Energy System

We present in Fig. (**3**), the first global view on the Multi-source Renewable Energy System, which consists of four blocks connected to each other. This system consists of four blocks interconnected. The first block includes the different energy sources that deal with the production of electrical energy. The second block, which has the characteristic of having a link with the other blocks, consists of the transmission devices, such as the bus of transmission and inverters. The third block is that of storage which one will find inside the various types of storage of energy such the battery. At the end the block of consumption which gathers the consumers.

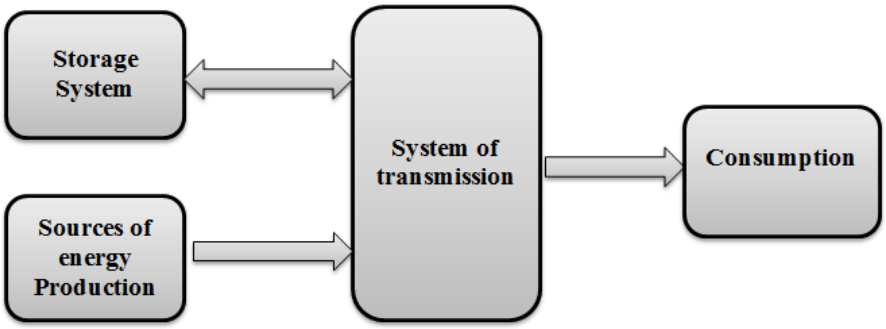

Fig. (3). Composition of Multi-source renewable energy system.

Fig. (**4**) describes a Multi-source Renewable Energy System to study. It consists of Photovoltaic module, Wind turbine, Inverter, AC/DC converter and a DC bus. In addition to one storage system of energies (a battery), all these components are connected to a Load.

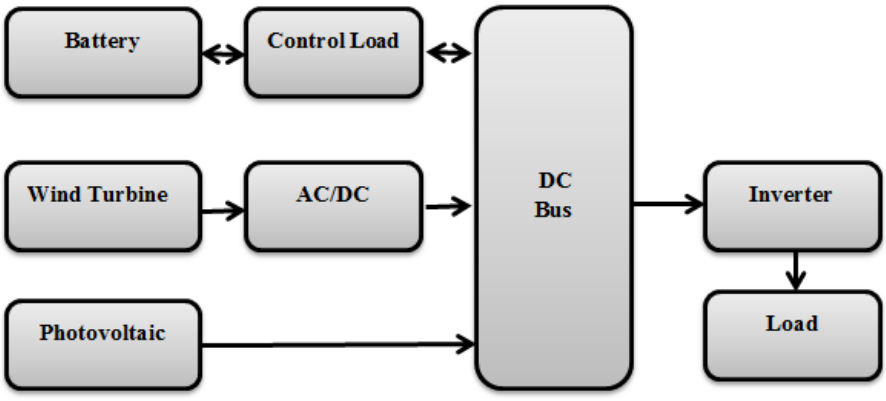

Fig. (4). Multi-source renewable energy system

To study the reliability of this system, we develop a model using the Deterministic Stochastic Petri Net (DSPN) depicted in Fig. (**5**).

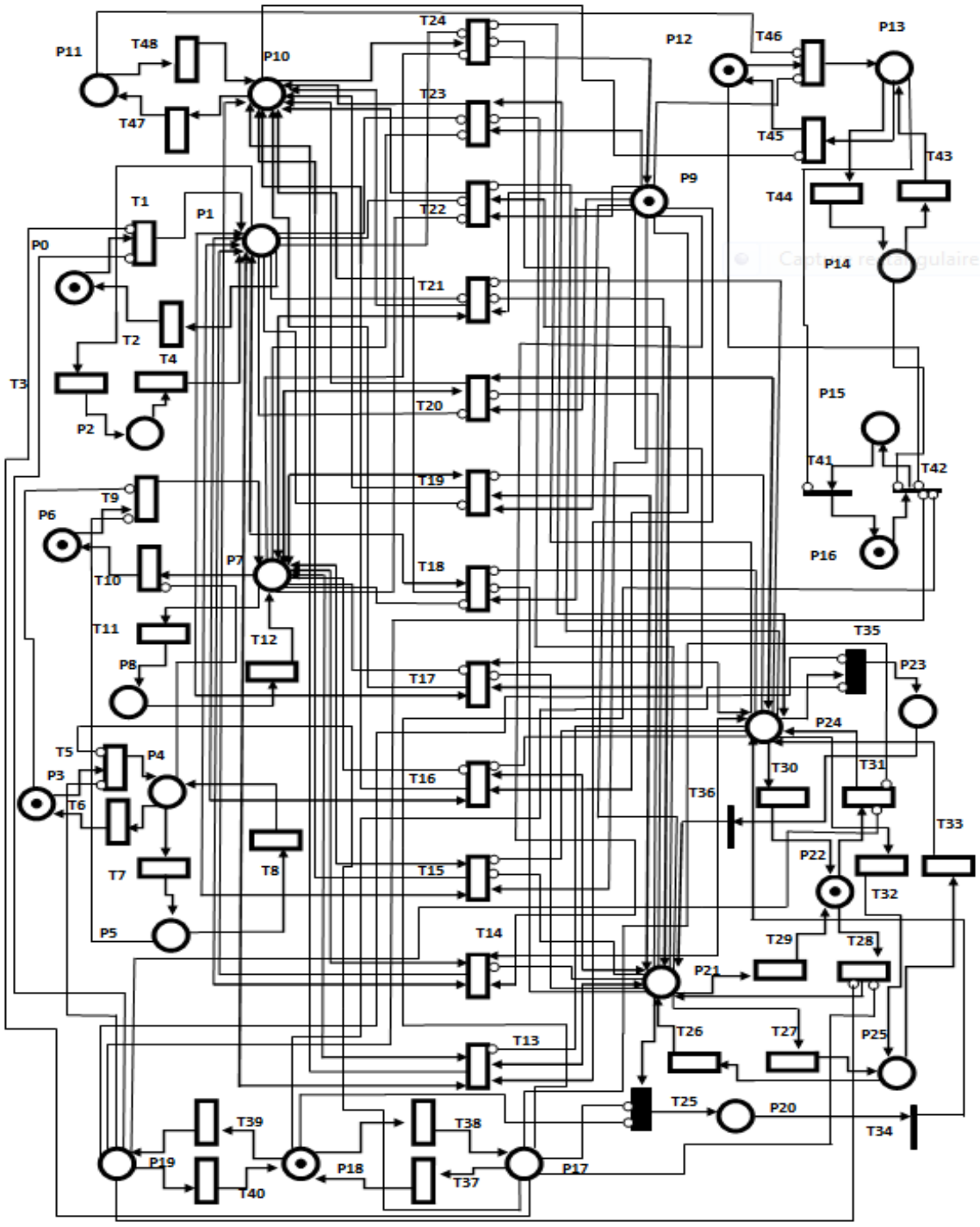

Fig. (5). Model DSPN of Multi-source renewable energy systems depicted in Fig. (**4**).

Table 5. Interpretation of places of the model DSPN depicted in Fig. (5).

Place	Signification
P0	Photovoltaic module is in wait state
P1	Photovoltaic module is in operating condition
P2	Photovoltaic module is in a breakdown state of
P3	Wait state of the wind turbine
P4	Operating condition of the wind turbine
P5	Breakdown state of the wind turbine
P6	Wait state of the AC/DC converter to connect wind to the DC bus

(Table 5) contd.....

Place	Signification
P7	Operating condition of the AC/DC converter to connect wind to the DC bus
P8	Breakdown State of the AC/DC converter to connect wind to the DC bus
P9	DC bus is free (vacuum)
P10	DC bus is occupied
P11	DC bus is in a breakdown state
P12	Wait state of Inverter
P13	Functional state of Inverter
P14	Breakdown State of Inverter
P15	Load is in connected state
P16	Load is in disconnected state
P17	Value max of load of the battery (Vmax)
P18	Value Vmin < V0 < Vmax
P19	Value min of discharge of the battery (Vmin)
P20	Stopped state of load of the battery
P21	Load state of the battery
P22	Wait state of the battery
P23	Stopped state of discharge of the battery
P24	Discharge of the battery
P25	Breakdown State of the battery

Table 6. Interpretation of transitions of the model DSPN depicted in Fig. (5).

Transition	Type	Signification
T1	stochastic	Passage the wait state towards the functional state of the photovoltaic
T2	stochastic	Return of photovoltaic of the functional state towards the wait state
T3	stochastic	Passage of the photovoltaic towards the breakdown state
T4	stochastic	Repair of photovoltaic
T5	stochastic	Passage of the wait state towards the functional state of the wind turbine
T6	stochastic	Return of the wind turbine of the functional state towards the wait state
T7	stochastic	Passage of the wind turbine towards the breakdown state
T8	stochastic	Repair of the wind turbine
T9	stochastic	Passage of the wait state towards the functional state of the AC/DC converter
T10	stochastic	Return of the AC/DC converter of the functional state towards the wait state
T11	stochastic	Passage of the AC/DC towards the state of breakdown
T12	stochastic	Repair of the AC/DC
T13, T14, T15, T16, T17, T18, T19, T20, T21, T22, T23.	stochastic	Passage of the DC bus of the state of vacuum towards the occupied state of DC bus
T24	stochastic	Return of the DC bus of the state occupied towards the vacuum state
T25	deterministic	Passage of load of the battery towards the stopping of the battery
T26	stochastic	Repair of the battery
T27	stochastic	Passage of the battery towards the breakdown state
T28	stochastic	Passage of the battery towards the load state
T29	stochastic	Return of the battery towards the wait state
T30	stochastic	Return of the battery towards the wait state
T31	stochastic	Passage of the battery towards the discharge state
T32	stochastic	Passage of the battery towards the breakdown state
T33	stochastic	Repair of the battery
T34	immediat	Return of the battery towards the discharge state
T35	deterministic	Passage of the battery of the state of discharge towards the stopped state
T36	immediat	Return towards the state of load of the battery
T37	stochastic	Passage of the value of the load (V) of Vmin towards Vmin<V<Vmax

(Table 6) contd.....

Transition	Type	Signification
T38	stochastic	Return of the value of the load (V) of Vmin <V< Vmax towards Vmin
T39	stochastic	Passage of the value of the load (battery) (V) of Vmin <V<Vmax towards Vmax
T40	stochastic	Return of the value of the load (battery) (V) of Vmax towards Vmin <V<Vmax
T41	immediat	Desactivation of the Load
T42	immediat	activation of the Load
T43	stochastic	Repair of the Inverter
T44	stochastic	Passage of inverter of the functional state towards the state of breakdown
T45	stochastic	Return of Inverter towards the wait state
T46	stochastic	Passage of Inverter towards the functional state
T47	stochastic	Passage of DC bus towards the breakdown state
T48	stochastic	Repair of the DC bus

In DSPN depicted in Fig. (**5**), before the beginning of the production, the Photovoltaic module, Wind turbine, AC/DC converter and Inverter are in wait state, represented by the presence of a token in places pp_3, p_6, p_{12} respectively. Such that the DC bus is in the free state (p_9) and the battery in wait state (p_{22}). This situation prevents the load to connecting itself. When one or both of the transitions t_5 and t_1 are fired, the wind turbine and the photovoltaic pass towards production state, are represented by p_4 and p_1. This operation will influence directly the other components of the system; the DC bus which will pass towards the occupied state (p_{10}) after firing one of the transitions (t_{13}, t_{14}, t_{15}, t_{16}, t_{17}, t_{18}, t_{19}, t_{20}, t_{21}, t_{22} and t_{23}), Inverter and the AC/DC converter which will also pass towards the functional state (p_{13}, p_7). This situation will influence directly the state of the Load which will pass from the disconnected state (p_{16}) to the connected state (p_{15}) after firing of the transition t_{42}.

The functioning of photovoltaic module and wind turbine separately or collectively allows the battery to pass through the load state represented by p_{21} in order to store the additional energy.

When the token is in place p_{17}, the load of the battery reaches its maximum value. The battery stops charging (p_{20}) when switching from photovoltaic module and a wind turbine to the breakdown state (p_2p_5) or in wait state (pp_3). In this case, battery ensures energy supply.

4. SIMULATION AND PERFORMANCE EVALUATION

In this part, we were interested in the performance evaluation of Multi-Source Renewable Energy Systems by using the DSPN. The Reliability and availability are the two performance indicators that will be analyzed by using the simulation software for Petri nets, known under the name TOTAL. This latter gives us the instant time of firing different transitions of DSPN.

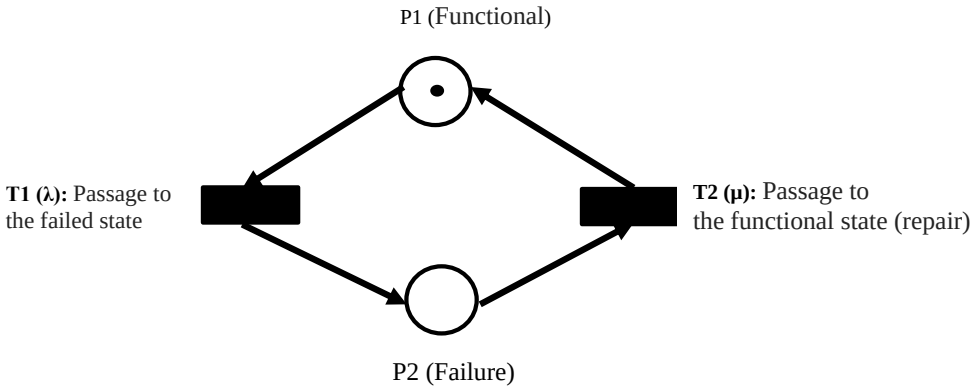

Fig. (6). Elementary DSPN modelling the functional state and failed state.

4.1. Principle

To study the reliability and availability of a component, we are interested only in the moment of the first switching from the functional state of the failed state (firing the transition T1), and the end time of the repair, *i.e.* switching from the failed state to the functional state, firing the transition T2 (Fig. **6**).

4.2. Graphic Illustration

The following graph illustrates the passage of a component from a functional state (= 1 binary) to the failed state (=0 binary) and vice-versa.

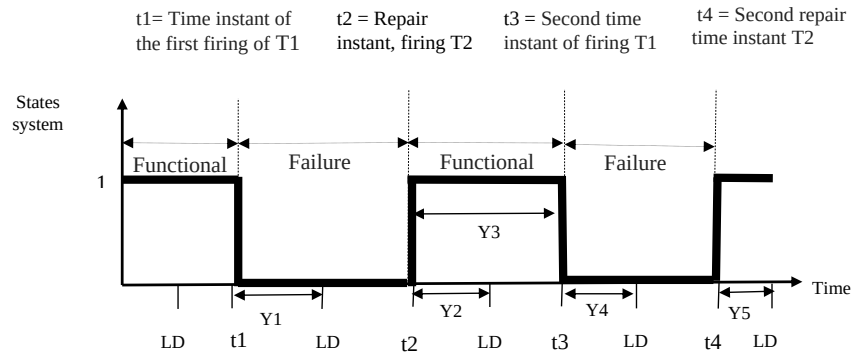

Remember that the different instants of switching from functional state to the fault state are given by the TOTAL simulation software and vice-versa.

4.3. Evaluation of Reliability (R)

In this work, we focus on the first firing of the transition T1 to quantify the reliability for *any given time instant* (LD).

4.4. Evaluation of Availability (A)

In the study of the availability, we are interested in firing transitions of failure and repair throughout the duration of the simulation.

The following diagram shows the different cases, depending on the value LD, in order to calculate the reliability and availability.

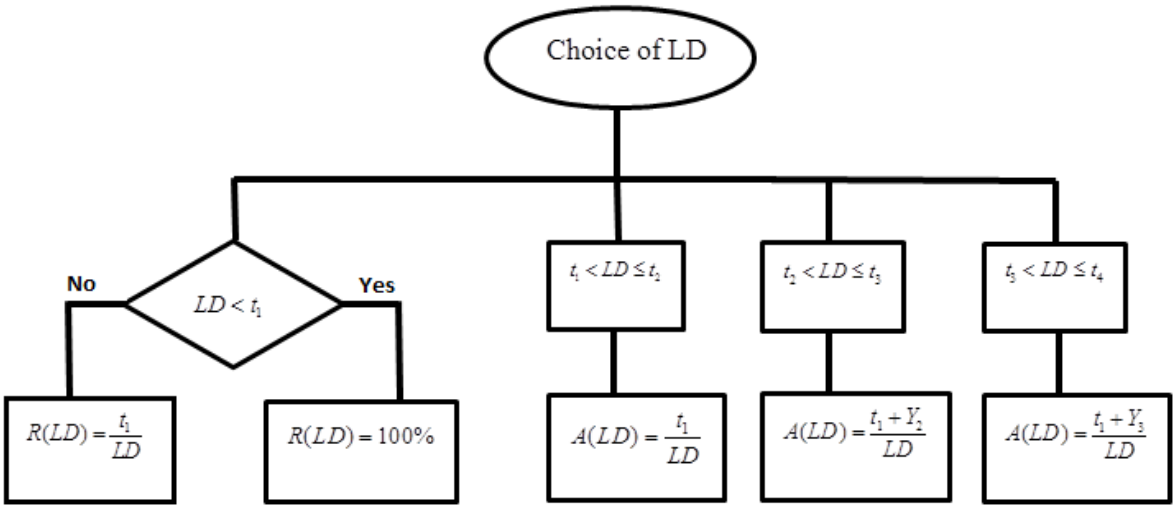

4.5. Parameters of Simulation

To be able to extract the results in this work using simulation on the Total software, we carried out simulation of the systems during 83220 hours (9,5 years). The parameters chosen for the systems of Figs. (**1b**, **2b** and **5**) are represented in the table below:

Table 7. Firing parameter associated with each transition.

Figure (1b)	Figure (2b)	Figure(5)
• **λ1**: 0,9 occ. h^{-1} • **λ2**: 0,1 occ. h^{-1} • (T3) Parameter of scale: 9,987.10^3, parameter of form: 3.9. • **μ4**: 0,00211855occ. h^{-1} • **λ5** : 10 occ. h^{-1} • **λ6** : 2 occ. h^{-1} • **λ7** : 9,51 . 10^{-6}occ. h^{-1} • **μ8** : 2,78 .10^{-3}occ. h^{-1} • **λ9** : 4,83.10^{-8}occ. h^{-1}. [35] • **μ10** : 5,21.10^{-3}occ. h^{-1} • **λ11** : 2, 2 occ. h^{-1} • **λ12** : 12 occ. h^{-1} • **λ14** : 2 occ. h^{-1} • **λ13** : 10 occ. h^{-1} • **λ15**: 9,51 . 10^{-6}occ. h^{-1} • **μ16**: 2,78 .10^{-3}occ. h^{-1}	• **λ1** : 5 occ. h^{-1}. • **λ2**: 0,0 occ. h^{-1}. • **λ3** :1,985.10^{-5}occ. h^{-1}. • **μ4** : 8,33. 10^{-3}occ. h^{-1}. • **λ5** : 4,83.10^{-8}occ. h^{-1}. • **μ6** : 5,21.10^{-3}occ. h^{-1}. • **λ7** : 2, 2 occ. h^{-1}. • **λ8** : 12 occ. h^{-1}. • **λ 9** : 2 occ. h^{-1}. • **λ10** : 10 occ. h^{-1}. • **λ11** : 9,51. 10^{-6}occ. h^{-1}. • **μ12** :2,78 .10^{-3}occ. h^{-1}.	• **λ1** : 5 occ. h^{-1}. • **λ2**: 0,09 occ. h^{-1}. • **λ3** : 1,985. 10^{-5}occ. h^{-1}. • **μ4** : 8,33. 10^{-3}occ. h^{-1}. • **λ1** : 0,9 occ. h^{-1}. • **λ2** : 0,1 occ. h^{-1}. • (T7) Parameter of scale: 9,987.10^3 , parameter of form: 3.9. • **μ8** : 0,00211855 occ. h^{-1}. • **λ 10** : 2 occ. h^{-1}. • **λ 9** : 10 occ. h^{-1}. • **λ 11** : 9,51 . 10^{-6}occ. h^{-1}. • **μ 12** :2,78 .10^{-3}occ. h^{-1}. • **λ47** : 4,83.10^{-8}occ. h^{-1}. • **μ48** : 5,21.10^{-3}occ. h^{-1}. • **λ24** : 2, 2 occ. h^{-1}. • **λ13… ,λ23** : 12 occ. h^{-1}. • **λ 45** : 2 occ. h^{-1}. • **λ 46** : 10 occ. h^{-1}. • **λ 44** : 9,51 . 10^{-6}occ. h^{-1}. • **μ 43** :2,78 .10^{-3}occ. h^{-1}. • (T 25). d = 2 *h*. • **μ 26** : 5,2E-3occ. h^{-1}. • **λ27**: 1E-5 occ. h^{-1}. • **λ28**: 0,1 occ. h^{-1}. • **λ29**:0,3 occ. h^{-1}. • **λ30**:0,4 occ. h^{-1}. • **λ31** :0,1 occ. h^{-1}. • **λ32** : 1E-5 occ . h^{-1}. • **μ 33**:5.2E-3occ. h^{-1}. • (T 35) : d = 3 *h*. • **λ37**:0,5 occ. h^{-1}. • **λ38** :0,7 occ. h^{-1}. • **λ39**:0,9 occ. h^{-1}. • **λ40**:0,8 occ. h^{-1}.

▪ Index “i” refers to transition “Ti”

▪ occ. h^{-1} correspond to occurrence per unit time

4.6. Results of Simulation

Fig. (**7a**) shows that the reliability of DC bus and the AC/DC is 100% throughout simulation contrary to the two other components (wind turbine, inverter). Their reliability reduced because of the firing of the transitions representing the passage towards the state of breakdown to t = 11986, 7 h (1, 37 years) and t= 35232, 1 h (4, 02 years).

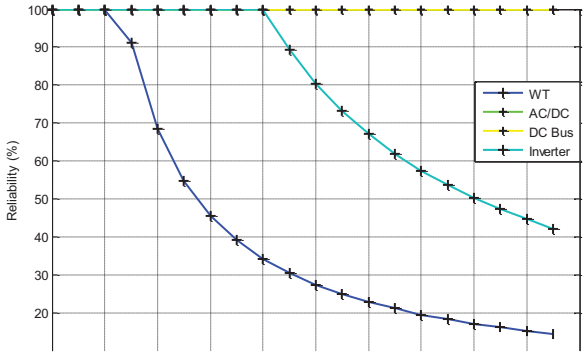

Fig. (7a). Reliability of each component for the Mono-source Energy System, with wind turbine only (system depicted in Fig. (**1a**)).

In Fig. (**7b**), the reliability of DC bus is 100% throughout simulation but for the two other components (inverter, photovoltaic), their reliability was stable at 100% until t= 20353,7 h (2,32 years) and t = 67195,4 H (7,67 years), respectively. Then it experienced a reduction because of the firing of the transitions of passage towards the state of breakdown.

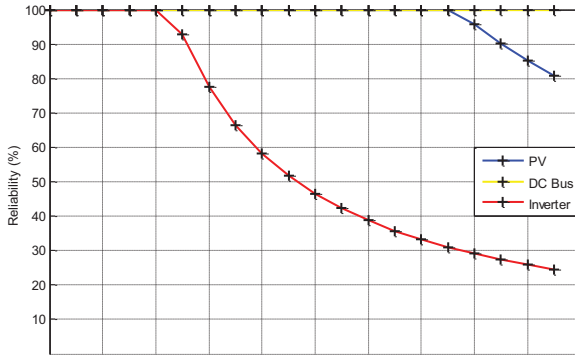

Fig. (7b). Reliability of each components of the Mono-source Energy System, with photovoltaic only (system depicted in Fig. **2a**)).

The total reliability which is represented in Fig. (**8a**) is stable with the value 100%. After the first year, it follows a reduction in its value to arrive to the value of 6% after 9.5 years of operation (83220 h).

On the other hand, the total reliability which is represented in Fig. (**8b**) is stable with the value 100%. After the second year, it follows a reduction in its value to reach the value of 19, 75%, after 9.5 years of operation (83220 h).

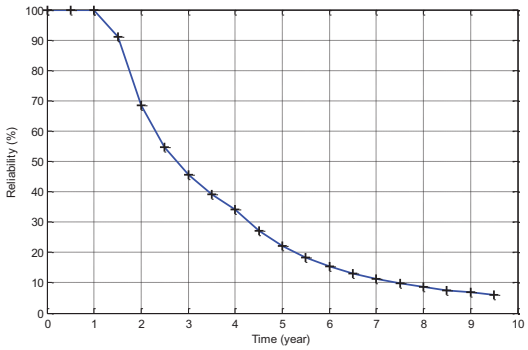

Fig. (8a). Total Reliability of the Mono-source Energy System with a wind turbine only (system depicted in Fig. (**1a**)).

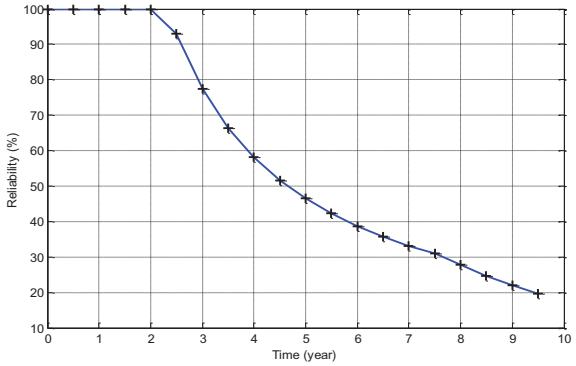

Fig. (8b). Total Reliability of the Mono-source Energy System, with photovoltaic only (system depicted in Fig. (**2a**)).

Fig. (**9a**) shows the reliability of the DC bus, photovoltaic module and battery which is 100% throughout simulation because of the absence of firing of the transitions, modelling the passage towards the state of breakdown. On the other hand, for three other components, their reliability was stable at 100% until t = 16253h (1,86years) for wind turbine, T =19639, 4 h (2, 24 years) for the inverter, and t = 77470, 9h (8, 84 years) for AC/DC. It then reduced because of the firing of the transitions which indicate the passage towards the state of breakdown.

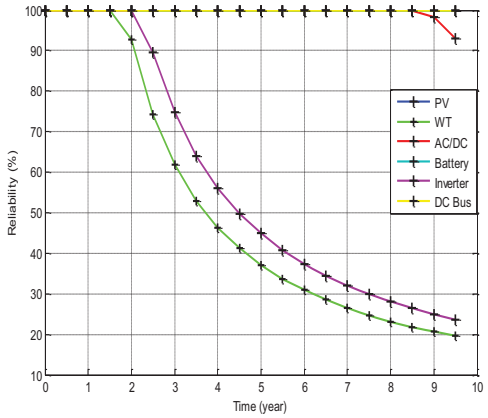

Fig. (9a). Reliability of each component of the Multi-Source Renewable Energy System (system depicted in Fig. (**4**)).

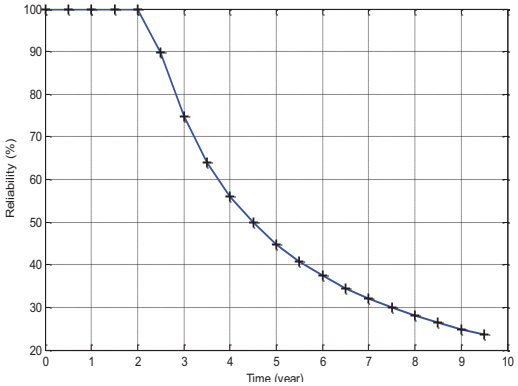

Fig. (9b). Total Reliability of the Multi-Source Renewable Energy System (system depicted in Fig. (**4**).

For the total reliability which is represented in Fig. (**9b**), it has been stable but the only difference is in the manner of its reduction which was slower than the preceding one, showing thatits value was 19.75% after 9.5 years of operation (83220 h).

In Fig. (**10a**), the availability of photovoltaic module, DC Bus and battery is stable with the value of 100% throughout the simulation. This stabilization is due to the absence of failure for this length of time. On the other hand, the availability of the wind turbine remains stable with the value 100% until the first shooting of the transition from failure; then its value caned tops and bottoms. This situation is due to the presence of 4 shootings of the transition from

failure to t = (16253 h, 32903,6 h, 48823 h, 68026,6h) and 4 shootings of the transition from repair to t = (16450,9 h, 34051,6 h, 48839,1 h, 69435 h). The value of availability of component AC/DC was stable at 100% until t = 8, 84 years (77470, 9 h) and that is only the first shooting of the transition from failure, then it followed a fall up to the value of 99.5% of the availability with the precision that the time of shooting of the transition from repair was equal to t = 77853,3 h. The inverter has a value of availability fixed at 100% until the first shooting of the transition from failure to t = 2,24 years (19639,4 h) after which it fell up to the minimal value with t = 2.5 years which was around 99.29%. It then increase exponentially by specifying that the moment of shooting of the transition from repair was around t = 19794,7 h.

In Figs. (**10b**, **11a**), and **11b**), we present the evolution of the total availability of the systems represented in Figs. (**1a**, **2a** and **4**), respectively, according to time. This availability is calculated by the application of the values of the availability of each component according to its architecture. The total availability of the system depicted in Figure 1a is represented by the graph, enabling us to divide the readings into four parts. The first: beginning until the first year when the system of was reliable having 100%, in the second part: the reading goes down again until the fourth year when its value was around 97.5%. The third part: between the fourth and the fifth year, it is around 96.5%. The fourth share: it remains stable until the end of simulation which is around 95%. The total availability which is represented in Figure 11b system of Figure 2a is stable, having its maximum value (100%) until the second year and a half. Then it undergoes a decline to reach the value of 96-68%. Afterward it follows an increase in an exponential way until the end of simulation. For the total availability which is represented in Figure 10b system of Figure 4, he shape of the graph is the same as that in Figure (11b), with the only difference of a decline in the availability to the value of 99.29%.

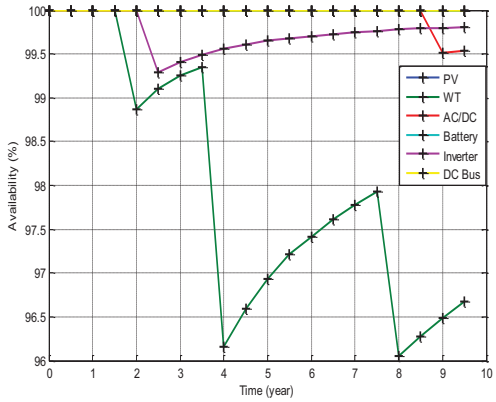

Fig. (10a). The Availability of each component of the Multi-Source Renewable Energy System (system depicted in Fig. (**4**)).

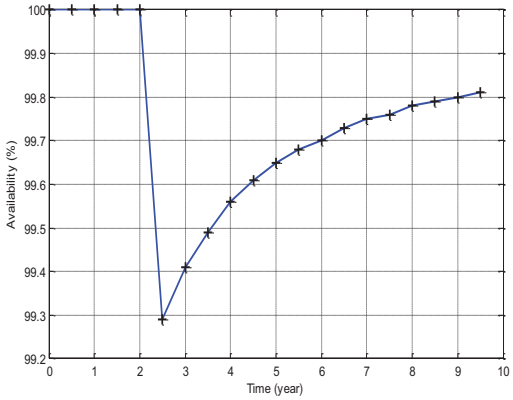

Fig. (10b). The total Availability of the Multi-Source Renewable Energy System(system depicted in Fig. (**4**)).

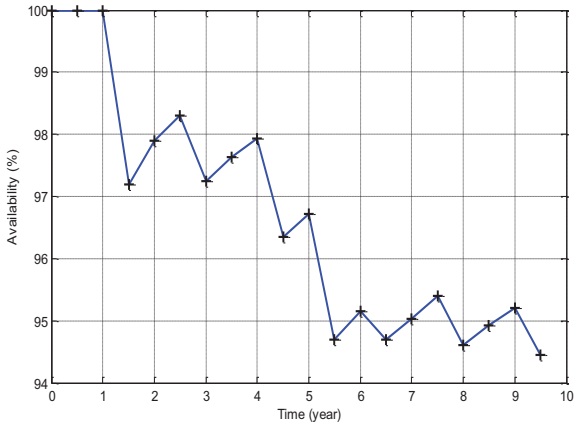

Fig. (11a). Total Availability of a Mono-source Energy System (with wind turbine only).

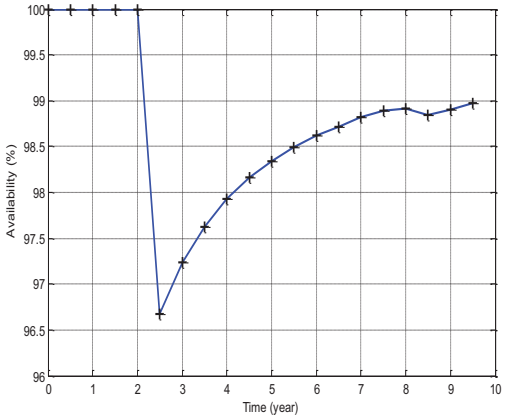

Fig. (11b). The total Availability of the Mono-source Energy System (with photovoltaic only).

4.7. Comparison of results

From the values obtained during simulation, we let us can leave there with the following comparison and results:

Considering reliability of the three systems which are represented in Figs. (**1a**, **2a**, and **4**). the system of **4** is better reliable compared to two others. The system of Fig. (**2a**) is better reliable than the system of Fig. (**1a**). Concerning the availability of the three systems which is represented in Figs. (**1a**), **2a** and in **4**). Broadly they have a good availability but the system of Fig. (**2a**) is a little better than the rest of the two . On the economic plan, the system of Fig. (**2a**) is the system least expensive compared to the system of Fig. (**3**). The complexity the system of Fig. (**3**) is high which makes it difficult to install, contrary to the system of Fig. (**2a**) which is smaller and simpler to install.

CONCLUSION

In this article, we developed two types of energy systems containing renewable resources (mono-source, multi sources). We began with the qualitative analysis (functional and dysfunctional, of waiting) of each system then calculated their performances (analyses quantitative) over one duration of time of 9.5 years and by precisely calculating the reliability and availability of each component, we measured reliability and total availability of these system containing the method which we developed. In end, we compared the results obtained to draw appropriate conclusions.

CONSENT FOR PUBLICATION

Not applicable.

CONFLICT OF INTEREST

The authors declare no conflict of interest, financial or otherwise.

ACKNOWLEDGEMENTS

Declared none.

REFERENCES

[1] K. Shivarama Krishna, and K. Sathish Kumar, "A review on hybrid renewable energy systems", *Renew. Sustain. Energy Rev.,* vol. 52, no. December, pp. 907-916, 2015.
[http://dx.doi.org/10.1016/j.rser.2015.07.187]

[2] N.L. Panwar, and S.C. Kaushik, "Surendra Kothari Role of renewable energy sources in environmental protection: A review", *Renew. Sustain. Energy Rev.,* vol. 15, no. 3, pp. 1513-1524, 2011.
[http://dx.doi.org/10.1016/j.rser.2010.11.037]

[3] R. David, and H. Alla, *Du Grafcet aux réseaux de Petri.,* Editions Hermès: Paris, 1992.

[4] C.A. Petri, Kommunikation mit Automaten. PhD thesis, University of Bonn, Bonn, West Germany, 1962.

[5] C.G. Cassandras, and S. Lafortune, *Introduction to Discrete Event Systems.,* 2nd ed Springer, 2007.

[6] O. Daniel, "les réseaux de Petri stochastiques pour l'évaluation des attributs de la sûreté de fonctionnement des systèmes manufacturiers", *Grenoble : sn.,* 1995.

[7] R. Zijal, Discrete Time Deterministic and Stochastic Petri Nets. In: G. Hommel, e.d, *Proc. Int. Workshop - Quality of Communication-Based Systems*, pp. 123{136, TU-Berlin, Germany, Sept. 1994. Kluwer.

[8] B.C. Wang, and M. Sechilariu, "F. Locment Power flow Petri Net modelling for building integrated multi-source power system with smart grid interaction", *Math. Comput. Simul.,* vol. 91, no. May, pp. 119-133, 2013.
[http://dx.doi.org/10.1016/j.matcom.2013.01.006]

[9] "D, Mirandol. R and Merseguer. J « QoS and energy management with Petri nets: A Self-adaptive framework", *J. Syst. Softw.,* vol. 85, pp. 2796-2811, 2012.
[http://dx.doi.org/10.1016/j.jss.2012.04.077]

[10] J. Li, "Meng Chu Zhouc, Tao Guoa,b, YahuiGana, Xianzhong Dai Robust control reconfiguration of resource allocation systems with Petri nets and integer programming", *Automatica,* vol. 50, pp. 915-923, 2014.
[http://dx.doi.org/10.1016/j.automatica.2013.12.015]

[11] D.L.U.H.F. Akham, T. Zhou, and T. Zhou, "Application of petri nets for the energy management of a photovoltic based power station including storage units renewable energy", *Franaxois,* pp. 1115-1124, 2010.

[12] A. Villemeur, *Sûreté de fonctionnement des systèmes industriels,* Eyrolles: France, 1988. ISBN-13: 978-2212016154.